



Published in final edited form as:

Mol Cell Neurosci. 2018 April ; 88: 33–42. doi:10.1016/j.mcn.2017.12.002.

Munc18-1 haploinsufficiency impairs learning and memory by reduced synaptic vesicular release in a model of Ohtahara syndrome

Albert Orock^{1,2,3}, Sreemathi Logan^{1,2,3}, and Ferenc Deak^{1,2,3,4,5,*}

¹Oklahoma Center for Neuroscience, Univ. Oklahoma Health Sciences Center, Oklahoma City, OK, USA

²Reynolds Oklahoma Center on Aging, Univ. Oklahoma Health Sciences Center, Oklahoma City, OK, USA

³Dept. of Geriatric Medicine, Univ. Oklahoma Health Sciences Center, Oklahoma City, OK, USA

⁴Dept. of Physiology, Univ. Oklahoma Health Sciences Center, Oklahoma City, OK, USA

⁵Harold Hamm Diabetes Center, Univ. Oklahoma Health Sciences Center, Oklahoma City, OK, USA

Abstract

Ohtahara syndrome, also known as type 4 of Early Infantile Epileptic Encephalopathy with suppression bursts (EIEE-4) is currently an untreatable disorder that presents with seizures and impaired cognition. EIEE-4 patients have mutations most frequently in the *STXBP1* gene encoding a Sec protein, *munc18-1*. The exact molecular mechanism of how these *munc18-1* mutations cause impaired cognition, remains elusive. The leading haploinsufficiency hypothesis posits that mutations in *munc18-1* render the protein unstable leading to its degradation. Expression driven by the healthy allele is not sufficient to maintain the physiological function resulting in haploinsufficiency. The aim of this study has been to understand how *munc18-1* haploinsufficiency causes cognitive impairment seen in EIEE-4. Here we present results from behavioral to cellular effects from a mouse model of *munc18-1* haploinsufficiency. *Munc18-1* heterozygous knock-out mice showed impaired spatial learning and memory in behavior tests as well as reduced synaptic plasticity in hippocampal CA1 long-term potentiation. Cultured *munc18-1* heterozygous hippocampal neurons had significantly slower rate of synaptic vesicle release and decreased readily releasable vesicle pool compared to wild-type control neurons in fluorescent FM dye assays. These results demonstrate that reduced *munc18-1* levels are sufficient to impair learning and memory by reducing neurotransmitter release. Therefore, our study

*Corresponding author: Ferenc Deak, M.D., Ph.D., Reynolds Oklahoma Center on Aging, Department of Geriatric Medicine, University of Oklahoma HSC, 975 N. E. 10th Street, SLY-BRC 1309-B, Oklahoma City, OK 73104-5419, Ph: (405) 271-8000, Ext. 47817, FAX: (405) 271-2298, Ferenc-Deak@ouhsc.edu.

Disclosures

Authors report no financial conflict of interest.

Publisher's Disclaimer: This is a PDF file of an unedited manuscript that has been accepted for publication. As a service to our customers we are providing this early version of the manuscript. The manuscript will undergo copyediting, typesetting, and review of the resulting proof before it is published in its final citable form. Please note that during the production process errors may be discovered which could affect the content, and all legal disclaimers that apply to the journal pertain.

implicates munc18-1 haploinsufficiency as a primary cause of cognitive impairment seen in EIEE-4 patients.

Keywords

munc18-1; Ohtahara syndrome; Early Infantile Epileptic Encephalopathy with suppression bursts (EIEE-4); cognition; synaptic neurotransmission

1. Introduction

The disease group of epileptic encephalopathy was originally established to name various neurological disorders with severe, and commonly multiform and intractable seizures during brain maturation that are thought to contribute to the progressive psychomotor dysfunction. The two most important hallmarks of epileptic encephalopathy are seizures and intellectual disability. The concept of epileptic encephalopathies is based on the assumption that aggressive epileptogenic activity during brain maturation is the main causative factor of progressive cognitive and neuropsychological deterioration. This age-related epileptogenic phenotype is peculiar to the immature brain and varies significantly in accordance with the stage of brain maturity at the time of disease onset. In some cases, seizures may be reduced or completely cease by adolescence but leave residual cognitive impairment. Although the causes of epileptic encephalopathy have been suggested to arise from a very wide range of physiological deficits, from anoxia at birth to autoimmunity, the etiology of disease onset in many cases remains unresolved (idiopathic).

Early Infantile Epileptic Encephalopathy 4 (EIEE-4) with burst suppression also known as Ohtahara syndrome (Ohtahara et al. 1976, Beal et al. 2012), is a rare, severely progressive epileptic encephalopathy. It is the earliest appearing age-related encephalopathy, typically affecting newborns within the first three months of life and as early as ten days after birth (Chakova 1996, Ohtahara and Yamatogi 2003, Saitsu et al. 2008, Saitsu et al. 2012). The disorder typically presents as severe intellectual disability, intractable seizures, and low life expectancy (Yamatogi and Ohtahara 1981). Patients who live past two years, usually progress to other types of epileptic encephalopathies such as West syndrome and Lennox-Gastaut syndrome (Yamatogi and Ohtahara 1981, Beal et al. 2012). EIEE-4 has a characteristic burst suppression pattern on an EEG (burst activity followed by very little brain activity) (Yamatogi and Ohtahara 2002, Jain et al. 2013). Seizures that develop due to EIEE-4 are very difficult to control even with combination of anticonvulsive drugs (Yamatogi and Ohtahara 2002, Beal et al. 2012). Individuals with EIEE-4 also suffer from slow mental development resulting in severe intellectual disability and requiring constant care.

The exact etiology of EIEE has been elusive, until recently. Metabolic disorders and brain malformations were initially suspected as the cause of this disease (Gowda et al. 2015). However, recent genetic screenings revealed mutations in certain genes were more common in EIEE patients. Specifically, de novo mutations in the following genes, *STXBP1*, *SLC25A22*, *CDKL5*, *ARX*, *SPTAN1*, *PCDH19*, *KCNQ2*, *SCN2A* have been seen in patients with epileptic encephalopathy (Saitsu et al. 2008, Pavone et al. 2012). Notably,

patients with EIEE-4 most frequently have mutations in the gene encoding syntaxin-binding protein 1 (*STXBPI*) also known as munc18-1 (Saitou et al. 2008, Saitou et al. 2010, Stamberger et al. 2016).

Proteins from the Sec1/Munc18 and SNARE (soluble NSF attachment protein receptor) families drive membrane fusion, a conserved mechanism that is important in intracellular membrane trafficking and exocytosis. In neurons action potentials induce neurotransmission by exocytosis of synaptic vesicles. Transmitter release involves a series of steps that include vesicle docking to the plasma membrane, priming to a release ready state, and calcium-triggered membrane fusion. The calcium signal-triggered neurotransmitter release provides the basic mechanism for communication among neurons, which is essential for information processing in the brain. At neuronal synapses munc18-1 interacts with these three SNAREs to drive vesicular release of transmitters: syntaxin-1, SNAP-25, and synaptobrevin/vesicle associated membrane protein. The three SNAREs produce fusion by forming tight four-helix bundles called SNARE complexes that bring the synaptic vesicle and plasma membranes together enabling transmitter release. Munc18-1 was initially linked to synaptic vesicle fusion based on its tight binding to syntaxin-1 in the so-called closed conformation that blocks its participation in SNARE complex formation (Rizo and Südhof 2002, Südhof and Rothman 2009). Therefore, it was postulated that munc18 had an inhibitory role in exocytosis. Recent findings in models with munc18-1 deletion contradicted this view. In munc18-1 KO mice synaptic release is completely abrogated (Verhage et al. 2000), just the opposite of what one would expect with disinhibition caused by eliminating an inhibitory factor. The expression level of munc18-1 is reduced to zero in the null mutant and to 50% in the heterozygous KO brain at E18 (Verhage et al. 2000, Toonen et al. 2005).

Munc18-1 binding to the SNARE complex is essential for SNARE associated exocytosis from the presynaptic terminal (Verhage et al. 2000). Deletion of munc18-1 in animals is embryonic lethal due to the complete lack of neurotransmitter secretion (Verhage et al. 2000, Deák et al. 2009). Individuals with EIEE-4 were found to have deletions and mostly *de novo* heterozygous missense mutations along the gene that encodes Munc18-1 (Saitou et al. 2008). These mutations are suspected to lead to unstable products which are degraded or aggregated (Chai et al. 2016) leading to haploinsufficiency, where the remaining unaffected *STXBPI* allele is unable to produce enough protein leading to aberrant neurophysiology (Saitou et al. 2010, Hager et al. 2014). The mechanism by which these mutations cause EIEE-4 is not clear but the current theories suggest impairments in neurotransmission may be the primary cause of EIEE-4. Looking at one of the major symptoms of EIEE-4, intellectual disability, it is possible that seizures associated with the disorder are destroying vital areas of the brain for learning and memory. Importantly, encephalopathy cases with cognitive impairment have been reported, which are caused by mutations in munc18-1 gene, however, some patients do not seize (Hamdan et al. 2011, Gburek-Augustat et al. 2016).

It is well established that synaptic plasticity is the basic process responsible for learning and memory in the brain (Dragoi et al. 2003, Neves et al. 2008) via modification of synaptic transmission and information processing in neuronal networks. The effects of reduced munc18-1 levels on learning and memory remain elusive. Based on this information we designed a set of experiments to test whether the impaired cognition associated with EIEE-4

is directly caused by deficits in neuronal transmission and not by seizure-induced neurodegeneration. We hypothesized that reduction in the expression levels of munc18-1 could lead to aberrant neurotransmission and hence compromise synaptic plasticity which, in turn, leads to impaired cognition. In order to test this hypothesis, we used munc18-1 heterozygous knockout mice (munc18-1^{+/-}) to model haploinsufficiency. We performed behavioral assays to measure their learning and memory, long-term potentiation experiments *ex vivo* and synaptic strength assays *in vitro* to understand how decreased levels of munc18-1 can cause deficits in learning and memory.

2. Material and methods

2.1 Animals

We used munc18-1 heterozygous (munc18-1^{+/-}) knockout animals that were generated as previously described (Verhage et al. 2000). Munc18-1^{+/-} line was maintained and experimental cohorts generated by breeding munc18-1^{+/-} with 129/SV (WT; Charles River Laboratories) mice. These animals did not suffer from spontaneous seizures, nor did they show any sign of seizure activity during video recorded behavioral assays when compared to WT littermates. Animals were housed in the Rodent Barrier Facility at the University of Oklahoma Health Sciences Center (OUHSC) on a 12-hour light/dark cycle and fed standard rodent chow (D12450B Research Diets Inc., New Brunswick, NJ) *ad libitum*. Experiments were conducted according to the National Institutes of Health's Guide for the Care and Use of Laboratory Animals and our protocols were approved by the Institutional Animal Care and Use Committee of OUHSC.

2.2 Genotyping

Munc18-1^{+/-} were genotyped using the methodology described in (Verhage et al. 2000, Deák et al. 2009). Briefly, a small piece of the tail was digested using a REDEXTRACT-N-Amp Tissue PCR kit (Sigma Aldrich, St. Louis, MO). Primers and PCR conditions were the same as described in (Verhage et al. 2000, Deák et al. 2009).

2.3 Hippocampal cultures

Heterozygous knockout pups were generated by breeding heterozygous knockout animals with wildtype animals. Hippocampal neurons from P0–P2 mice were dissociated using trypsin (5mg/ml for 10 mins at 37°), triturated with a siliconized Pasteur pipette, and plated onto 12-mm coverslips coated with Matrigel (~12 coverslips/hippocampus). Neurons were cultured at 37°C in a humidified incubator with 95% air and 5% CO₂ for at least 12 days *in vitro* in minimal essential media containing 5g/L glucose, 0.1g/L transferrin, 0.25g/L insulin, 0.3g/L glutamine, 5–10% FBS, 2% B-27 supplement, and 1 μM cytosine arabinoside as described (Deák et al. 2009).

2.4 Behavioral assays

2.4.1 Radial Arm Water Maze (spatial memory assessment)—We tested spatial learning and memory using a modified radial arm water maze (RAWM) protocol previously described (Shukitt-Hale et al. 2004). Briefly, animals were moved to the behavior room at least 48 hours before the test to habituate. An eight-arm radial maze was filled about 2/3rds

with an opaque fluid (water with food coloring). Different intra-maze visual cues (geometrical shapes) were placed at the ends of each arm above the water. A platform was submerged around 2 cm below the surface of the water (hidden platform). On day 1 of the experiment, the mice were habituated to the hidden platform for 15 seconds before being returned to their cages. The animals were then placed at the end of an arm without the platform and then allowed to swim for 60 seconds to find and get on the non-visible platform. The animals were left on the platform for 15 seconds and then returned to their cages. Animals which could not find the platform at the end of the 60 seconds were carefully guided to the platform. After all animals had gone through the procedure, the experiment was repeated 7 more times (8 trials per day; Acquisition). Experimenters were blinded to the genotype of the mouse and the starting arm for each animal was randomized. At the end of the 8th trial, the animals were returned to their cages. This procedure was repeated for two more days. After day 3, the animals were returned to their home cages and left undisturbed for one week. A week later, a probe test was performed. The animals were tested in the RAWM (4 trials per animal) if they could still remember (recall) the location of the platform. Animal movements in the maze were recorded by a camera and their path analyzed using an automated tracking system (Noldus Ethovision XT 11, Wageningen, The Netherlands). The swim speed, distance covered, time to target and errors were recorded. An error was counted when the animal's full body-length entered into an arm which did not have the platform.

2.4.2 Intellicage (Reversal learning assessment)—Reversal learning, a form of cognitive flexibility was assessed using a complex cohabitate environment called an Intellicage (New Behavior AG, Zurich, Switzerland). For detailed description of the apparatus, we refer to a previous paper (Galsworthy et al. 2005). Briefly, the whole apparatus of Intellicage fits into a large standard rat cage (Techniplast, model 2000). It has four chambers in the corners of the cage with a chip reader at the entrance to the chambers. Water bottles were placed in the corner chambers. Two days before the test, the animals were subcutaneously injected with micro transponders which were programmed into the chip-readers of the Intellicage. The intellicage requires minimum handling after the experiment has begun and allowed the animals to socialize with each other, which should reduce stress on the animals. The procedure used is a modified protocol previously described in (Too et al. 2016). Mice were allowed to drink water from any corner for two days (habituation and acclimation). After the habituation, the transponders in the animals were randomly programmed to allow access to water from only one corner. Visiting the wrong corner was registered as an error and the gate closed preventing access to water. This place learning was continued for two more days. Animals which could not find the right corner and appeared to be in distress from lack of water were removed and excluded from the test (four WT controls and five *munc18-1^{+/-}* animals). Once all the animals had learned the corner they could drink water from, the place learning task was stopped and the transponders were programmed to the opposite corner. This part is called as the reversal task and tests the animals' cognitive flexibility. The reversal task was performed for two more days to allow time for the animal to learn the new location of the accessible water source before the experiment was stopped and the animals returned to their original cages. The mice were

assessed based on the number of times the animal went to the correct *vs.* incorrect corners and is expressed as a percentage of all corner visits.

2.5 Electrophysiology

Long-term potentiation (LTP) measurements—To measure the effects of *munc18-1* haploinsufficiency on long-term potentiation, the cellular mechanism of learning and memory, we adapted our protocol previously described (Liu et al. 2014). Brains were carefully removed from euthanized mice and put in ice cold oxygenated artificial cerebrospinal fluid (ACSF) solution containing (in mM: NaCl 126, KCl 2.5, NaH₂PO₄ 1.25, MgCl₂ 2, CaCl₂ 2, NaHCO₃ 26, glucose 10, pyruvic acid 2, ascorbic acid 0.4) for approximately one minute. Appropriate portions of the brain were trimmed away and the base was cut at an approximate 20-degree angle. The brain was then fixed to an ice-cold stage and placed in a HM650V vibrating microtome (Thermo Scientific, Burlington, ON, USA) filled with chilled cold oxygenated slicing solution containing (in mM): sucrose 240, NaCl 25, KCl 2.5, NaH₂PO₄ 1.25, NaHCO₃ 26, ascorbic acid 0.4, glucose 10, MgCl₂ 10, pyruvic acid 2. The brain was sliced horizontally and hippocampal slices of thickness 350 μ m were collected and transferred to a recovery chamber containing oxygenated ACSF. The slices were left in this chamber at 32°C for 30 minutes and then room temperature for 30 minutes to recover. To record, the slice was transferred to and positioned on a P5002A multi-electrode array (Alpha MED Scientific Inc., Osaka, Japan). The chamber was perfused with oxygenated ACSF at a rate of 2 mL/min, at 32°C. Field excitatory post synaptic potentials (fEPSPs) were generated in the CA1 region of the hippocampus by stimulating downstream electrodes in the CA1 and CA3 regions of the hippocampus along the Schaffer collateral pathway. Input/output curves (I/O curves) were generated by applying increasing stimulus currents to the pathway from 0–100 μ A to the pathway and recording the responses. The threshold stimulus for generating fEPSPs was determined as 50% of the stimulus strength needed to generate the maximum fEPSP amplitude during the I/O curve measurement. The slice was stimulated once every 30 seconds until a stable baseline lasting at least 10 minutes was observed. Long-term potentiation was induced using a tetanus (high frequency stimulation train of 100 pulses at 100Hz applied 4 times with 30 second intervals). Immediately after the tetanus we resumed baseline stimulation and recorded fEPSPs for at least 60 more minutes. Finally, we recorded another I/O curve generated as described above. For all recordings, we used the MED-64 system and Mobius software (Alpha MED Scientific Inc.). Potentiation was calculated as the percent increase of the mean fEPSP descending slope (10–90 section) after high-frequency stimulation and normalized to the mean fEPSP descending slope of baseline recordings during 3 minutes prior tetanus. In order to assess the synaptic facilitation we induced a second identical stimulus 50ms after the first for baseline recording. We calculated the Paired Pulse Facilitation (PPF) ratio by dividing the amplitude of the second response by that of the first one. We have recorded LTP from 5 *munc18*^{+/-} mice and 8 WT controls. Most of these animals were not tested in any other assay before, while 3 *munc18*^{+/-} and 2 WT mice were randomly selected from the RAWM assay cohort.

2.6 Synaptic Release Recording by FM Imaging

Fluorescence imaging experiments were carried out using a modified protocol as previously described (Deak et al. 2004). Briefly, a modified Tyrode solution containing (in mmol/L): 150 NaCl, 2.5 KCl, 2 MgCl₂·6H₂O 10 glucose, 10 HEPES and 2 CaCl₂·2H₂O at pH 7.4 was used as bath solution. Synaptic boutons were loaded with FM1-43 (16 μM; Molecular Probes, Eugene, OR) or FM2-10 (400 μM) for 90 s in a hyperkalemic solution of 90mM K⁺ (bath Tyrode solution with concentrations of NaCl and KCl changed to 60mM and 90mM respectively) before being washed away with calcium-free Tyrode bath solution to minimize spontaneous release. All staining and washing protocols were performed in the presence of 10 μM of 6-cyano-7-nitro-quinoxaline-2,3-dione (CNQX) and 50 μM of (2R)-amino-5-phosphonopentanoate (AP-5) to prevent recurrent activity. After the wash, synaptic boutons (about 1μm²) were selected (at least 100 boutons per coverslip). Synaptic vesicle fusion and release was induced by gravity perfusion of Tyrode solution. In the case of full synaptic recycling, FM1-43 was used to label the synapses and high K⁺ Tyrode solution was perfused for 60 seconds before being washed with calcium-free Tyrode for another 60 seconds. This process was repeated 4 more times (to ensure complete release of all fluorescence). To measure the readily releasable pool of vesicles, FM2-10 was used to label the synapses, and a high sucrose supplemented (500mM) Tyrode solution was used to induce vesicle fusion and release by creating an osmotic gradient which released just the readily releasable pool of vesicles. After the sucrose challenge followed by a wash for 2 minutes with calcium-free Tyrode solution we used high KCl stimuli to release the recycling pool of vesicles. During these stimulations, the loss of fluorescence in the selected synaptic boutons (measure of synaptic release) was captured by a cooled CCD camera (Roper Scientific, Trenton, NJ) and analyzed using Metafluor Software (Universal Imaging, Downingtown, PA). The data for release rate was then normalized to starting fluorescence intensity to help compare large and small synapses for release properties as expressed in the histograms.

2.7 Western blotting

To quantify the amount of munc18-1, half brains from controls (WT) and munc18-1^{+/-} KO mice were lysed in RIPA buffer (Sigma Aldrich) containing protease inhibitor cocktail (Roche Diagnostics, Mannheim, Germany), sonicated and the supernatant was collected and protein concentration was determined using a DC protein quantification assay kit (BioRad). All antibodies used in Western blots were from commercial sources with well-established and public validation data as indicated by the catalog numbers and referenced to the Antibody Registry (see next paragraph for registry ID numbers).

Equal amounts of total protein (20μg) from each brain lysate were separated on a 10% bis-tris gel (Novex), blotted on to a nitrocellulose membrane (BioRad), and blocked with blocking buffer (5% BSA in 1X Tris Buffered Saline with 0.1% tween (TTBS)). The membrane was then sequentially probed with primary antibodies for munc18-1 (rabbit polyclonal anti-munc18-1; Synaptic Systems Cat# 116 002, Antibody Registry: RRID:AB_887736) and actin (mouse anti-actin; Millipore Cat# MAB1501, RRID:AB_2223041) in blocking buffer (1:2000 in 1% BSA blocking buffer) overnight. The membrane was washed and incubated with the secondary antibody, donkey anti-rabbit, 800CW (LI-COR Biosciences Cat# 926-32213, RRID:AB_621848) for munc18-1 and goat

anti-mouse 680CW for actin (LI-COR Biosciences Cat# 827-08364, RRID:AB_10793856) (1:10000 in TTBS) for one hour at room temperature. The membrane was visualized using an Odyssey imager (Li-Cor, Lincoln Nebraska). Munc18-1 levels were analyzed from pixel densities and normalized to actin levels.

2.8 Chemicals

The chemicals used in this study were obtained from the following sources: FM 2–10, FM1-43, B-27 supplement and MEM (Invitrogen, Carlsbad, CA), Matrigel and FBS (Thermofisher, Waltham, MA) and transferrin (Millipore, Billerica, MA). All other chemicals were purchased from Sigma Aldrich.

2.9 Statistics

Significance was calculated using Student's t-test, repeated measures 2-way ANOVA with p values ($p < 0.05$ marked as *, $p < 0.01$ as ** for RAWM, Intellicage, LTP) and Kolmogorov–Smirnov test (K-S test, Fluorescence assays). Results are displayed as Mean \pm S.E.M.

3. Results

3.1 Munc18-1 haploinsufficiency causes impaired spatial learning and memory in mice

We chose the *munc18^{+/-}* mice as an ideal model to test the effect of *munc18-1* haploinsufficiency on learning and memory functions separately from seizures, as we did not observe any major seizure episodes in the *munc18-1^{+/-}* animals. First, to assess the impact of deleting one allele of *STXBP1* gene we quantified the expression levels of *munc18-1* in the brains of adult heterozygous mice and compared them to controls. Using Western blotting we found that brains from heterozygous animals expressed about 25% less *munc18-1* protein than WT controls (Fig. 1A). Next, we assessed the spatial learning and memory performance of the *munc18-1^{+/-}* mice in the radial arm water maze (RAWM) assay. We followed the standard design and conducted RAWM assay with two parts, first about learning a specific location (the acquisition phase) and second the recall of this information to find the same location one week after the acquisition phase (recall of spatial memory). While the WT and *munc18-1^{+/-}* started out the acquisition phase at the same level, by day 3 of the training, the *munc18-1^{+/-}* animals were making significantly more errors than WT controls (2.9 ± 0.4 errors, for 6 month-old female *munc18-1^{+/-}* animals $n=9$ versus 1.3 ± 0.2 errors, for WT $n=8$; $p < 0.01$ repeated measures 2-way ANOVA; Fig. 1B, C). Consistent with these results, during the probe test, *munc18-1^{+/-}* animals performed significantly worse than WT controls (3.8 ± 0.7 errors, $n=9$ for *munc18-1^{+/-}* animals versus 2.0 ± 0.4 errors, $n=8$ for WT; $p < 0.01$ repeated measures 2-way ANOVA; Fig. 1D). *Munc18-1^{+/-}* animals also traveled a longer distance before finding the platform by day 3 (Fig. 1E) as well as on the probe day (Fig. 1F), mirroring the results we saw from the errors made. It is worthy to note that WT animals swam significantly faster (14.7 ± 0.7 cm/s on day 3; 13.1 ± 1 cm/s on the probe day) than the *munc18-1^{+/-}* animals (7.9 ± 0.3 cm/s on day 3; 8.2 ± 0.5 cm/s on the probe day) during the test ($p < 0.001$; repeated measures 2-way ANOVA). This movement speed difference did not affect the results because the animals still found the platform within the time limit (60s) and by counting errors and distance traveled as our readout the phenotype observed is not influenced by swim speed.

We also used a complex cohabitate environment called as Intellicage (Fig. 2A) to measure the animals' learning and memory flexibility. Our assay had again two parts: acquiring proper information about a location (place learning by finding the right corner to access drinking water) and as second task learning a different location (reversal) (Fig. 2A). The Intellicage is designed to keep the mice social and limit human interaction with the mice in order to maintain a less stressful environment. Again, six month-old mice were used for this assay. In the acquisition phase, there was no significant difference in the error rates between WT and *munc18-1^{+/-}* animals ($43.37 \pm 10.12\%$ and $32.78 \pm 7.75\%$, respectively) (Fig. 2B). During the reversal part of this assay, when water was available only from the opposite corner to original location, *munc18-1^{+/-}* animals perform significantly worse (errors of $82.85 \pm 8.06\%$; $n=7$) than WT controls ($56 \pm 11.77\%$; $n=7$) (Fig. 2C; $p < 0.05$ 1-tailed t-test) indicating a deficit in working and spatial memory.

3.2 Munc18-1 haploinsufficiency impairs long-term potentiation in the hippocampus

As stated earlier, *munc18-1* deletion in homozygote mice disrupts synaptic transmission leading us to hypothesize that altered synaptic transmission is the mechanism behind the cognitive impairment seen in patients of EIEE-4 and here that we have observed in *munc18-1* heterozygous mice. To investigate the effects of reduced *munc18-1* expression on the synaptic function in learning and memory, we performed long-term potentiation (LTP) assays. LTP refers to the phenomenon of persistent increase in the strength of synapses after strong activation. It is typically induced by high frequency stimulations. We collected hippocampal slices from young (5–9 months old) *munc18-1* heterozygous animals and induced LTP along the Schaffer collateral pathway connecting CA3 to CA1 of the hippocampus, an important pathway in spatial learning and memory (Dragoi et al. 2003) (Fig. 3A). LTP was successfully induced in both WT and *munc18-1^{+/-}* animals using high frequency stimulation (Fig. 3D). However, level of potentiation was significantly reduced in *munc18-1^{+/-}* animals ($147.0 \pm 1.5\%$; $n=5$) compared to WT controls ($232.3 \pm 1.7\%$; $n=8$) (Fig. 3D; $p < 0.001$) one hour after induction, indicating an impairment in LTP.

To measure the properties of neurotransmission in these hippocampal slices, we measured the fEPSPs at baseline and after LTP induction in response to stepwise increased stimuli (5–100 μ A). On input/output curves (I/O) from these data (Fig. 3E) WT animals showed a significant increase in their response after LTP induction at all stimulus intensities; however, we recorded a significantly attenuated potentiation of the response after LTP in the *munc18-1^{+/-}* slices (Fig. 3E), a sign of impaired synaptic plasticity. We also measured the changes in the fiber volley (presynaptic input) in both groups across the same range of stimuli. We did not see a significant change in the fiber volley at baseline and after LTP for either group (data not shown).

Next, we analyzed short-term synaptic plasticity at these synapses and calculated the Paired Pulse Facilitation (PPF) as ratio between synaptic responses to a double-pulse stimulation with 50 ms interval. There were no significant differences in the PPF between the groups either before or after LTP induction (Fig. 3C) showing neural facilitation, a form of short-term plasticity that is exclusively presynaptic, is not affected by *munc18-1* haploinsufficiency.

3.3 Munc18-1 haploinsufficiency impairs neurotransmitter release

Based on the key role of munc18-1 in synaptic neurotransmitter release, we decided to investigate the effects munc18-1 haploinsufficiency on synaptic vesicle release dynamics. We cultured primary hippocampal neurons from munc18-1^{+/-} animals and loaded synapses with the fluorescent dye FM1-43 (Fig. 4A, B). After individual fluorescent synaptic puncta were selected, we measured their fluorescence change during depolarizing stimulation (Fig. 4C) to analyze the dynamics of synaptic vesicle release. We measured the rate of fluorescence loss during the first 15 seconds of stimulation and showed that the munc18-1^{+/-} cultures had a significantly slower rate of synaptic vesicle release when compared to WT neurons (Fig. 4D). The munc18-1^{+/-} neurons released about 25% less fluorescence than WT synapses ($p < 0.001$; K-S test). Next, to find the mechanism for slower release in munc18-1^{+/-} animals, we assessed the size of readily releasable pool (RRP) of synaptic vesicles.

3.4 Munc18-1 haploinsufficient neurons have reduced readily releasable pool (RRP) of synaptic vesicles

Considering Munc18-1 is essential for vesicle docking and priming, we decided to investigate whether munc18-1 haploinsufficiency affects the readily releasable pool of vesicles. The RRP is the vesicle pool which is already docked and primed at the active zone.

In order to selectively activate these vesicles, we applied a hypertonic Tyrode solution containing 500 mM sucrose as described in the methods. This revealed that munc18-1^{+/-} neurons had a significantly smaller readily releasable pool size (0.17 ± 0.002 normalized fluorescence for munc18-1^{+/-}) when compared to control (0.19 ± 0.003) WT neurons (Fig. 5A, B; $P < 0.001$ K-S Test). To further analyze the release kinetics in munc18^{+/-} neurons, after depletion of RRP with sucrose stimulation, we allowed the synapses to recover for 90 seconds and stimulated them with strong depolarization using the 90 mM KCl protocol. Release rates of munc18-1^{+/-} neurons was 26% slower even under these circumstances when compared to WT control neurons (Fig. 5C; $p < 0.001$ K-S Test). The ratio of the second, depolarization-induced release to RRP was similar in WT and munc18-1^{+/-} mice (241% \pm 21 and 209% \pm 11, respectively), which is consistent with the primary effect of munc18 haploinsufficiency on reducing RRP.

4. Discussion

The key finding in this study is that munc18-1 haploinsufficiency causes cognitive impairment. In order to model haploinsufficiency, we used heterozygous animals with one of the munc18-1 alleles deleted. Surprisingly, munc18-1 levels were reduced only by 25% in these heterozygous animals, instead of about 50% as expected from reports on munc18-1 levels in embryonic brain from heterozygous KO mice at E18 (Verhage et al. 2000, Toonen et al. 2005). In a recent study, (Patzke et al. 2015) munc18-1 levels were found to be ~70% after selective disruption of one allele of the STXBPI gene, which is in good accordance with our results here. Interestingly, despite the munc18-1 levels in the munc18-1^{+/-} mice being higher than expected, our tests clearly indicated that there was a significant decline in spatial learning and memory in these animals, further illustrating the importance of munc18-1 in cognition. Our behavioral assay (Intellicage) showed munc18-1^{+/-} animals can

adequately perform a place learning task as well as wild-type controls in a relatively stress-free environment. Interestingly, these same animals have difficulties learning the reversal task on the same system. These results show that reducing *munc18-1* by 25% does not completely ablate learning. However, in more complex tests such as the RAWM, or the reversal task in the Intellicage, reduced expression of *munc18-1* negatively impacts learning and memory, suggesting impairments in synaptic plasticity. It is worth noting that the RAWM was chosen as an alternate behavioral test not because it is more stressful to the animals but because it is more sensitive than the Intellicage. In the RAWM test, the animals have a smaller chance of finding the correct choice by accident (12.5% vs 25% in the Intellicage). Conceptually, impaired synaptic plasticity would explain the cognitive impairment exhibited by the *munc18-1^{+/-}* animals during the behavioral assays. Spatial learning and memory critically depends on hippocampal tri-synaptic information processing (Neves et al. 2008, Bannerman et al. 2014, Hartley et al. 2014, Moser et al. 2015). Indeed, we found that *munc18-1* haploinsufficiency mediated cognitive impairment seen in these animals by markedly reducing hippocampal CA1 LTP. Analyzing synaptic properties using I/O curves before and after LTP induction, we saw that reduction in *munc18-1* expression causes impairments in plasticity despite maintained baseline synaptic strength in CA1.

To understand the underlying mechanism behind reduced LTP and cognitive impairments, we measured the release rates of *munc18-1^{+/-}* neurons. To achieve this we used detailed analysis of release parameters from hundreds of individual synapses by live fluorescence imaging with FM dye. We found that *munc18-1^{+/-}* neurons had a reduced synaptic vesicle release rate, and this was due to a reduced readily releasable pool size. After depleting the RRP, further stimulation of the neurons using a depolarizing stimulation, revealed basically unchanged phenotype in *munc18-1^{+/-}* neurons, which is a sign that their RRP was effectively replenished similarly to WT neurons. However, due to reduced *munc18-1* expression, the *munc18-1^{+/-}* neurons still had a smaller RRP than WTs and their release rates then lag significantly behind WT neurons (Fig. 5D).

The limited effect of *munc18-1* haploinsufficiency on RRP is somewhat surprising, as *munc18^{-/-}* neurons have a complete arrest of vesicular neurotransmission. We want to point to the relatively modest decrease of *munc18-1* levels in heterozygous knockout brains (to 75%) as possible explanation. Although at first it may look as not a dramatic synaptic phenotype, but the reduced RRP size and slower release of vesicles strongly indicate that *munc18* levels are rate limiting for synaptic neurotransmission. We assume that the better sensitivity of our direct detection of well identified presynaptic vesicular release by fluorescence probes provide an advantage compared to electrophysiological methods depending on indirect probing via post-synaptic currents induced by all synaptic connections onto the given neuron (Patzke et al. 2015). As it was shown by us and others, *munc18-1* interacts with the SNARE complex (Dulubova et al. 2007, Deák et al. 2009, Pertsinidis et al. 2013) and this marked effect on release rate and RRP size could be explained by such an interaction. Taken together, *munc18-1* haploinsufficiency induced reduction in RRP and slower neurotransmitter release emerges as the underlying cause of impaired spatial learning and memory seen in these animals. These results implicate *munc18-1* haploinsufficiency as a primary cause of mental retardation seen in EIEE-4.

EIEE-4 is a life threatening disorder with no effective treatment. In the few rare cases when seizures were controlled by antiepileptic drugs, cognitive development was still significantly delayed (Fusco et al. 2001, Sivaraju et al. 2015). The neurological clinical field has been disturbed for long time by repeatedly finding very little correlation between seizure onset, seizure severity, and the degree of intellectual disability in these patients (Saitu et al. 2010, Milh et al. 2011, Stamberger et al. 2016). Finding an answer is further complicated by the fact that currently no drug is available to effectively combat the disorder. In light of the role of munc18-1 in the pathophysiology of EIEE-4, it should also be noted that both in humans and animal models munc18-1 mutations produce the strongest phenotype compared to mutations in other SNARE associated proteins, especially in the context of hippocampal learning and memory. It is evident in this study as we saw that reducing the expression of munc18-1 by only 25% is sufficient to cause the severe and strong phenotype exhibited by these animals. Mutations in other SNARE associated proteins like munc13 and complexin can lead to ataxia (Netrakanti et al. 2015) and deficits in social behavior (Drew et al. 2007), respectively, but the phenotype is not as strong as what is reported with munc18-1 mutations. Interestingly, recent detailed analysis of movements in children with munc18 mutations revealed ataxia-like symptoms (Milh et al. 2011). One possible explanation for this may be that other genes in the brain are able to compensate, at least partially, for the loss of these other SNARE associated proteins and in the process, they retains some functionality of the original SNARE proteins and present with not-so-severe symptoms. As there is no good alternative to munc18-1 in the brain and hence any disruption in munc18-1 expression will result in significant pathophysiological effects.

To the best of our knowledge, this study is the first to implicate munc18-1 haploinsufficiency as the primary cause of cognitive impairment seen in EIEE-4. Further experiments will need to be carried out to determine the role played by munc18-1 haploinsufficiency in the seizure phenotype seen in EIEE-4. Gaining mechanistic insight into how munc18-1 haploinsufficiency causes the symptoms of EIEE-4 will lead to understanding the etiology of the disorder and will help in developing effective therapies to prevent cognitive impairment and other symptoms of the disorder.

5. Conclusion

We provide evidence which implicates munc18-1 haploinsufficiency as the primary cause of cognitive impairment seen in Ohtahara syndrome/EIEE-4. We show that munc18-1 haploinsufficient mice have impaired synaptic plasticity and reduced long-term potentiation in hippocampal CA1 region. Synaptic dysfunction is caused by less readily available synaptic vesicles for release. Thus, reduced munc18-1 levels in EIEE-4 cause severe enough synaptic dysfunction which ultimately manifests as cognitive deficit.

Acknowledgments

Munc18 KO mice were a kind gift from Dr. Thomas C. Südhof. We are grateful for the excellent technical help from Sima Asfa and Jennifer Fessler with the mouse husbandry and neuronal cultures. We thank Dr. Nikolett Szarka for her advice and practical help on establishing the cell cultures and PCR. We also thank Julie Farley and Matthew Mitschelen for their help with mouse husbandry and the establishment of behavioral assays. The advices on this project from Drs. Robert E. Anderson, Beverley Greenwood-Van Meerveld, Jose Rizo-Rey, William E. Sonntag and Rheal Towner (Graduate School Advisory Committee members to A.O.) are greatly appreciated.

Grant support. We thank the Presbyterian Health Foundation for a Seed grant (to FD) and the Oklahoma Center for Neuroscience for a Student Pilot grant (to AO). The research results discussed in this publication were also made possible in part by funding through the Health Research award for our project from the Oklahoma Center for the Advancement of Science and Technology (to FD) and the support of NIH P20GM104934 CoBRE Pilot grant (to FD).

References

- Bannerman DM, Sprengel R, Sanderson DJ, McHugh SB, Rawlins JNP, Monyer H, Seeburg PH. Hippocampal synaptic plasticity, spatial memory and anxiety. *Nat Rev Neurosci.* 2014; 15(3):181–192. DOI: 10.1038/nrn3677 [PubMed: 24552786]
- Beal JC, Cherian K, Moshe SL. Early-Onset Epileptic Encephalopathies: Ohtahara Syndrome and Early Myoclonic Encephalopathy. *Pediatric Neurology.* 2012; 47(5):317–323. doi: <http://dx.doi.org/10.1016/j.pediatrneurol.2012.06.002>. [PubMed: 23044011]
- Chai YJ, Sieracki E, Tomatis VM, Gormal RS, Giles N, Morrow IC, Xia D, Gotz J, Parton RG, Collins BM, Gambin Y, Meunier FA. Munc18-1 is a molecular chaperone for alpha-synuclein, controlling its self-replicating aggregation. *J Cell Biol.* 2016; 214(6):705–718. DOI: 10.1083/jcb.201512016 [PubMed: 27597756]
- Chakova L. On a rare form of epilepsy in infants--Ohtahara syndrome. *Folia Med (Plovdiv).* 1996; 38(2):69–73.
- Deak F, Schoch S, Liu X, Sudhof TC, Kavalali ET. Synaptobrevin is essential for fast synaptic-vesicle endocytosis. *Nat Cell Biol.* 2004; 6(11):1102–1108. DOI: 10.1038/ncb1185 [PubMed: 15475946]
- Deák F, Xu Y, Chang WP, Dulubova I, Khvotchev M, Liu X, Südhof TC, Rizo J. Munc18-1 binding to the neuronal SNARE complex controls synaptic vesicle priming. *J Cell Biol.* 2009; 184(5):751–764. [PubMed: 19255244]
- Dragoi G, Harris KD, Buzsáki G. Place representation within hippocampal networks is modified by long-term potentiation. *Neuron.* 2003; 39(5):843–853. [PubMed: 12948450]
- Drew CJ, Kyd RJ, Morton AJ. Complexin 1 knockout mice exhibit marked deficits in social behaviours but appear to be cognitively normal. *Hum Mol Genet.* 2007; 16(19):2288–2305. DOI: 10.1093/hmg/ddm181 [PubMed: 17652102]
- Dulubova I, Khvotchev M, Liu S, Huryeva I, Südhof TC, Rizo J. Munc18-1 binds directly to the neuronal SNARE complex. *Proc Natl Acad Sci U S A.* 2007; 104(8):2697–2702. [PubMed: 17301226]
- Fusco L, Pachatz C, Di Capua M, Vigeveno F. Video/EEG aspects of early-infantile epileptic encephalopathy with suppression-bursts (Ohtahara syndrome). *Brain Dev.* 2001; 23(7):708–714. [PubMed: 11701283]
- Galsworthy MJ, Amrein I, Kuptsov PA, Poletaeva II, Zinn P, Rau A, Vyssotski A, Lipp H-P. A comparison of wild-caught wood mice and bank voles in the Intellicage: assessing exploration, daily activity patterns and place learning paradigms. *Behavioural Brain Research.* 2005; 157(2): 211–217. doi: <http://dx.doi.org/10.1016/j.bbr.2004.06.021>. [PubMed: 15639172]
- Gburek-Augustat J, Beck-Woedl S, Tzschach A, Bauer P, Schoening M, Riess A. Epilepsy is not a mandatory feature of STXBPI associated ataxia-tremor-retardation syndrome. *Eur J Paediatr Neurol.* 2016; 20(4):661–665. DOI: 10.1016/j.ejpn.2016.04.005 [PubMed: 27184330]
- Gowda VK, Bhat A, Bhat M, Ramaswamy P. Ohtahara syndrome associated with hemimegalencephaly and intracranial lipoma. *J Pediatr Neurosci.* 2015; 10(2):185–187. DOI: 10.4103/1817-1745.159212 [PubMed: 26167232]
- Hager T, Maroteaux G, Pont P, Julsing J, van Vliet R, Stiedl O. Munc18-1 haploinsufficiency results in enhanced anxiety-like behavior as determined by heart rate responses in mice. *Behav Brain Res.* 2014; 260:44–52. DOI: 10.1016/j.bbr.2013.11.033 [PubMed: 24304718]
- Hamdan FF, Gauthier J, Dobrzyniecka S, Lortie A, Mottron L, Vanasse M, D’Anjou G, Lacaille JC, Rouleau GA, Michaud JL. Intellectual disability without epilepsy associated with STXBPI disruption. *Eur J Hum Genet.* 2011; ejhg2010183 [pii]. doi: 10.1038/ejhg.2010.183
- Hartley T, Lever C, Burgess N, O’Keefe J. Space in the brain: how the hippocampal formation supports spatial cognition. *Philos Trans R Soc Lond B Biol Sci.* 2014; 369(1635):20120510.doi: 10.1098/rstb.2012.0510 [PubMed: 24366125]

- Jain P, Sharma S, Tripathi M. Diagnosis and Management of Epileptic Encephalopathies in Children. *Epilepsy Research and Treatment*. 2013; 2013:9.doi: 10.1155/2013/501981
- Liu CC, Tsai CW, Deak F, Rogers J, Penuliar M, Sung YM, Maher JN, Fu Y, Li X, Xu H, Estus S, Hoe HS, Fryer JD, Kanekiyo T, Bu G. Deficiency in LRP6-mediated Wnt signaling contributes to synaptic abnormalities and amyloid pathology in Alzheimer's disease. *Neuron*. 2014; 84(1):63–77. DOI: 10.1016/j.neuron.2014.08.048 [PubMed: 25242217]
- Milh M, Villeneuve N, Chouchane M, Kaminska A, Laroche C, Barthez MA, Gitiaux C, Bartoli C, Borges-Correia A, Cacciagli P, Mignon-Ravix C, Cuberos H, Chabrol B, Villard L. Epileptic and nonepileptic features in patients with early onset epileptic encephalopathy and STXBP1 mutations. *Epilepsia*. 2011; 52(10):1828–1834. DOI: 10.1111/j.1528-1167.2011.03181.x [PubMed: 21770924]
- Moser MB, Rowland DC, Moser EI. Place cells, grid cells, and memory. *Cold Spring Harb Perspect Biol*. 2015; 7(2):a021808.doi: 10.1101/cshperspect.a021808 [PubMed: 25646382]
- Netrakanti PR, Cooper BH, Dere E, Poggi G, Winkler D, Brose N, Ehrenreich H. Fast Cerebellar Reflex Circuitry Requires Synaptic Vesicle Priming by Munc13-3. *Cerebellum (London, England)*. 2015; 14(3):264–283. DOI: 10.1007/s12311-015-0645-0
- Neves G, Cooke SF, Bliss TV. Synaptic plasticity, memory and the hippocampus: a neural network approach to causality. *Nat Rev Neurosci*. 2008; 9(1):65–75. DOI: 10.1038/nrn2303 [PubMed: 18094707]
- Ohtahara S, Yamatogi Y. Epileptic encephalopathies in early infancy with suppression-burst. *J Clin Neurophysiol*. 2003; 20(6):398–407. [PubMed: 14734930]
- Ohtahara S, Yamatogi Y, Ohtsuka Y. Prognosis of the Lennox syndrome-long-term clinical and electroencephalographic follow-up study, especially with special reference to relationship with the West syndrome. *Folia Psychiatr Neurol Jpn*. 1976; 30(3):275–287. [PubMed: 992512]
- Patzke C, Han Y, Covy J, Yi F, Maxeiner S, Wernig M, Südhof TC. Analysis of conditional heterozygous STXBP1 mutations in human neurons. *The Journal of Clinical Investigation*. 2015; 125(9):3560–3571. DOI: 10.1172/JCI78612 [PubMed: 26280581]
- Pavone P, Spalice A, Polizzi A, Parisi P, Ruggieri M. Ohtahara syndrome with emphasis on recent genetic discovery. *Brain Dev*. 2012; 34(6):459–468. DOI: 10.1016/j.braindev.2011.09.004 [PubMed: 21967765]
- Pertsinidis A, Mukherjee K, Sharma M, Pang ZP, Park SR, Zhang Y, Brunger AT, Südhof TC, Chu S. Ultrahigh-resolution imaging reveals formation of neuronal SNARE/Munc18 complexes in situ. *Proc Natl Acad Sci U S A*. 2013; 110(30):E2812–2820. DOI: 10.1073/pnas.1310654110 [PubMed: 23821748]
- Rizo J, Südhof TC. Snares and Munc18 in synaptic vesicle fusion. *Nat Rev Neurosci*. 2002; 3(8):641–653. DOI: 10.1038/nrn898 [PubMed: 12154365]
- Saitsu H, Kato M, Matsumoto N. Haploinsufficiency of STXBP1 and Ohtahara syndrome. *Epilepsia*. 2010; 51:71–71. DOI: 10.1111/j.1528-1167.2010.02857.x [PubMed: 20618405]
- Saitsu, H., Kato, M., Matsumoto, N. Haploinsufficiency of STXBP1 and Ohtahara syndrome. *Jasper's Basic Mechanisms of the Epilepsies*. Noebels, JL, Avoli, M, Rogawski, MA, Olsen, RW., Delgado-Escueta, AV., editors. Bethesda (MD): National Center for Biotechnology Information (US); 2012.
- Saitsu H, Kato M, Mizuguchi T, Hamada K, Osaka H, Tohyama J, Uruno K, Kumada S, Nishiyama K, Nishimura A, Okada I, Yoshimura Y, Hirai S, Kumada T, Hayasaka K, Fukuda A, Ogata K, Matsumoto N. De novo mutations in the gene encoding STXBP1 (MUNC18-1) cause early infantile epileptic encephalopathy. *Nat Genet*. 2008; 40(6):782–788. DOI: 10.1038/ng.150 [PubMed: 18469812]
- Saitsu H, Kato M, Okada I, Orii KE, Higuchi T, Hoshino H, Kubota M, Arai H, Tagawa T, Kimura S, Sudo A, Miyama S, Takami Y, Watanabe T, Nishimura A, Nishiyama K, Miyake N, Wada T, Osaka H, Kondo N, Hayasaka K, Matsumoto N. STXBP1 mutations in early infantile epileptic encephalopathy with suppression-burst pattern. *Epilepsia*. 2010; doi: 10.1111/j.1528-1167.2010.02728.x
- Shukitt-Hale B, McEwen JJ, Szprengiel A, Joseph JA. Effect of age on the radial arm water maze—a test of spatial learning and memory. *Neurobiology of Aging*. 2004; 25(2):223–229. doi: [http://dx.doi.org/10.1016/S0197-4580\(03\)00041-1](http://dx.doi.org/10.1016/S0197-4580(03)00041-1). [PubMed: 14749140]

- Sivaraju A, Nussbaum I, Cardoza CS, Mattson RH. Substantial and sustained seizure reduction with ketogenic diet in a patient with Ohtahara syndrome. *Epilepsy & Behavior Case Reports*. 2015; 3:43–45. DOI: 10.1016/j.ebcr.2015.03.003 [PubMed: 26005637]
- Stamberger H, Nikanorova M, Willemsen MH, Accorsi P, Angriman M, Baier H, Benkel-Herrenbrueck I, Benoit V, Budetta M, Caliebe A, Cantalupo G, Capovilla G, Casara G, Courage C, Deprez M, Destree A, Dilena R, Erasmus CE, Fannemel M, Fjaer R, Giordano L, Helbig KL, Heyne HO, Klepper J, Kluger GJ, Lederer D, Lodi M, Maier O, Merkschlager A, Michelberger N, Minetti C, Muhle H, Phalin J, Ramsey K, Romeo A, Schallner J, Schanze I, Shinawi M, Slegers K, Sterbova K, Syrbe S, Traverso M, Tzschach A, Uldall P, Van Coster R, Verhelst H, Viri M, Winter S, Wolff M, Zenker M, Zoccante L, De Jonghe P, Helbig I, Striano P, Lemke JR, Moller RS, Weckhuysen S. STXBP1 encephalopathy: A neurodevelopmental disorder including epilepsy. *Neurology*. 2016; 86(10):954–962. DOI: 10.1212/WNL.0000000000002457 [PubMed: 26865513]
- Südhof TC, Rothman JE. Membrane fusion: grappling with SNARE and SM proteins. *Science*. 2009; 323(5913):474–477. [PubMed: 19164740]
- Too LK, Li KM, Suarna C, Maghzal GJ, Stocker R, McGregor IS, Hunt NH. Deletion of TDO2, IDO-1 and IDO-2 differentially affects mouse behavior and cognitive function. *Behavioural Brain Research*. 2016; 312:102–117. doi: <http://dx.doi.org/10.1016/j.bbr.2016.06.018>. [PubMed: 27316339]
- Toonen RF, de Vries KJ, Zalm R, Südhof TC, Verhage M. Munc18-1 stabilizes syntaxin 1, but is not essential for syntaxin 1 targeting and SNARE complex formation. *J Neurochem*. 2005; 93(6): 1393–1400. DOI: 10.1111/j.1471-4159.2005.03128.x [PubMed: 15935055]
- Verhage M, Maia AS, Plomp JJ, Brussaard AB, Heeroma JH, Vermeer H, Toonen RF, Hammer RE, van den Berg TK, Missler M, Geuze HJ, Südhof TC. Synaptic assembly of the brain in the absence of neurotransmitter secretion. *Science*. 2000; 287(5454):864–869. [PubMed: 10657302]
- Yamatogi Y, Ohtahara S. Age-dependent epileptic encephalopathy: a longitudinal study. *Folia Psychiatr Neurol Jpn*. 1981; 35(3):321–332. [PubMed: 7327468]
- Yamatogi Y, Ohtahara S. Early-infantile epileptic encephalopathy with suppression-bursts, Ohtahara syndrome; its overview referring to our 16 cases. *Brain Dev*. 2002; 24(1):13–23. [PubMed: 11751020]

Highlights

- Munc18-1 heterozygous mice (munc18^{+/-}) have impaired spatial learning and memory.
- Munc18^{+/-} mice have reduced long-term potentiation in hippocampal CA1 region.
- Synaptic dysfunction is caused by slower release of synaptic vesicles.
- Reduced munc18-1 level alone is sufficient to cause cognitive deficits in EIEE-4.

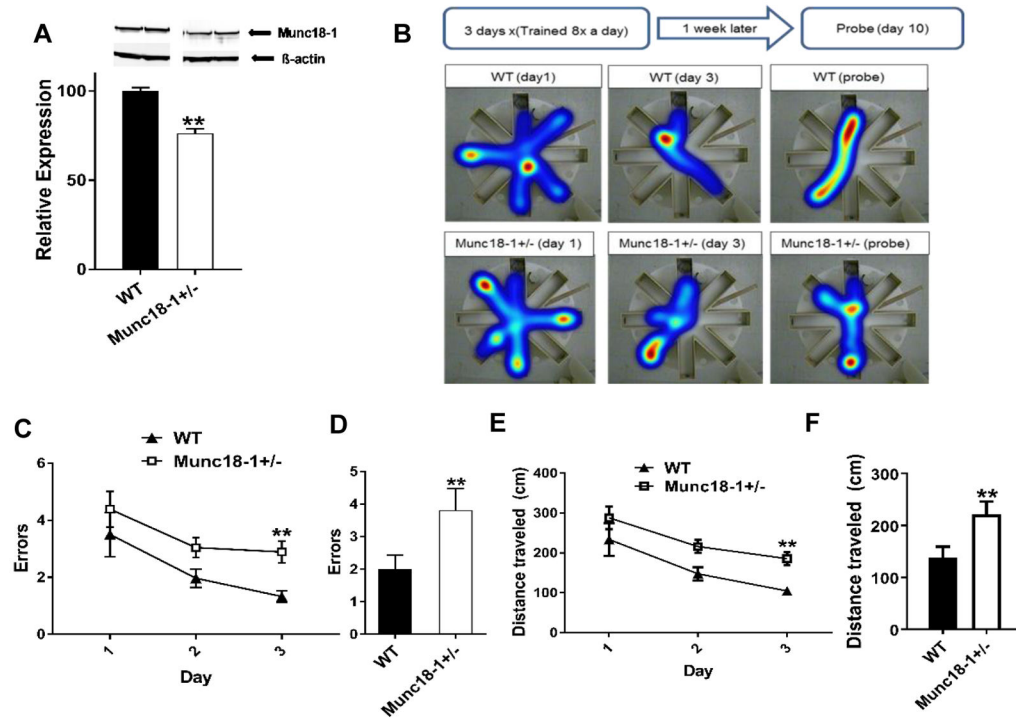
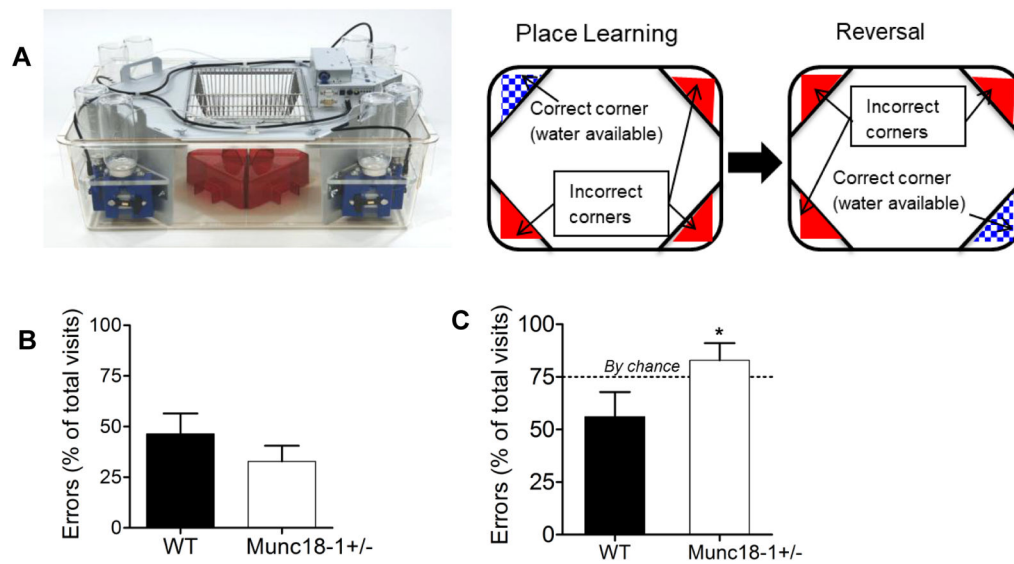


Fig. 1. Spatial learning and memory impairment in *munc18-1*^{+/-} mice. (A) Western blot data showing *munc18-1*^{+/-} animals express 25% less *munc18-1* than WT controls (WT= 100±1.96, n=6; *munc18-1*^{+/-} = 76.30±2.57, n=7; p<0.0001). (B) Illustration of experimental procedure and representative heat map data of WT and *munc18-1*^{+/-} mice in the RAWM. (C) Graph depicts errors made during acquisition phase. *Munc18-1*^{+/-} animals make significantly more errors (# of entries into the incorrect arm) by day 3 (2.9±0.4) of the acquisition when compared to WT animals (1.3±0.2) and (D) bar graph depicts that on the probe day, *munc18-1*^{+/-} animals again performed with more errors (3.8±0.7) when compared to WT animals (2±0.4). (E) *Munc18-1*^{+/-} animals covered more distance by day 3 (*munc18-1*^{+/-} = 185.7 ± 17.1 cm; WT= 104.7 ± 9.2 cm) and (F) also on the probe day (*munc18-1*^{+/-} = 221.3 ± 24.8 cm; WT= 138.2 ± 21.1 cm) compared to WT controls. (WT n=8, *munc18-1*^{+/-} n=9 mice; p=0.007 using 2-way RM ANOVA.

**Fig. 2.**

Learning deficits of *munc18*^{+/-} mice in Intellicage reversal task assay. (A) Picture of the Intellicage setup and illustration of the place learning and reversal paradigm. (B) Error rates of six-month-old *munc18-1*^{+/-} (n=7) and WT (n=7) animals during the place learning task in the Intellicage (calculated as [100*(number of incorrect visits/total number of visits)]). (C) Bar graph depicts the *munc18-1*^{+/-} animals' performance during the reversal task in the Intellicage with an error rate (82.9 ± 8.1%, n=7) significantly worse than WT (56 ± 11.8%, n=7), (p<0.05, 1-tailed t-test). Results are shown as Mean ± S.E.M.

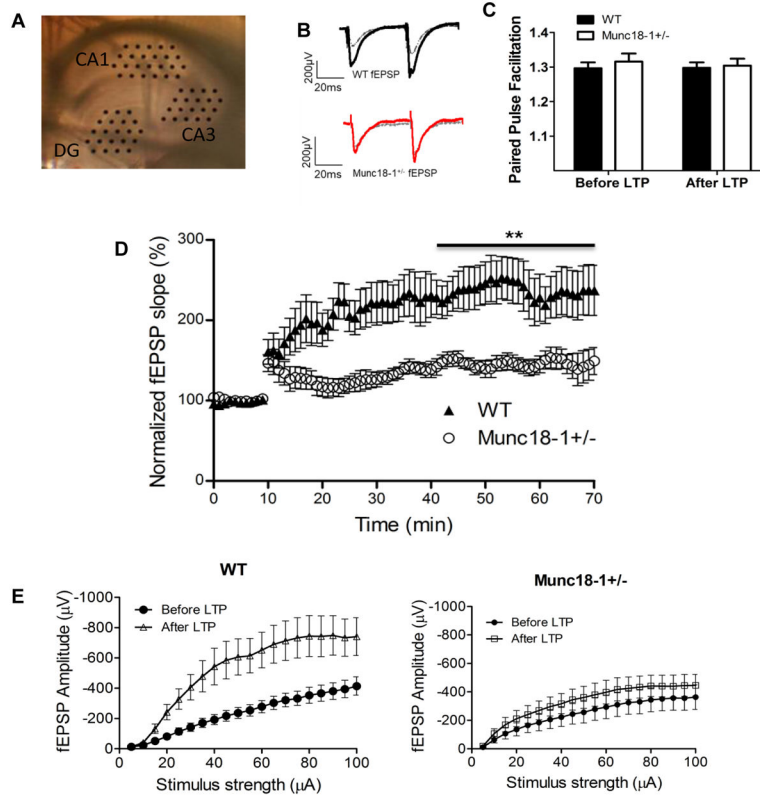


Fig. 3. Reduced synaptic potentiation of hippocampal CA1 synapses in *munc18*^{+/-} mice. (A) Picture of hippocampal slice in MED 64 probe with electrodes positioned on the dentate gyrus (DG), CA3 and CA1 regions. (B) Representative traces for *munc18-1*^{+/-} and WT before (dashed grey) and after (black for WT and red for *munc18-1*^{+/-}) LTP induction. (C) Ratio of amplitudes in paired pulse facilitation at 50 ms for both WT and *munc18-1*^{+/-} animals either before or 60 minutes after LTP. (D) Normalized fEPSP for both *munc18-1*^{+/-} (n=5 animals; 7 slices) and WT (n=8 animals; 10 slices) depicting *munc18-1*^{+/-} have impaired LTP ability (p<0.001; students t-test). (E) Input-output curves from CA1 region before (black) and after (red for *munc18-1*^{+/-} and blue for WT mice) LTP induction. Note that WT had a significantly higher response after LTP induction. *Munc18-1*^{+/-} show only minor increase in the response after LTP induction.

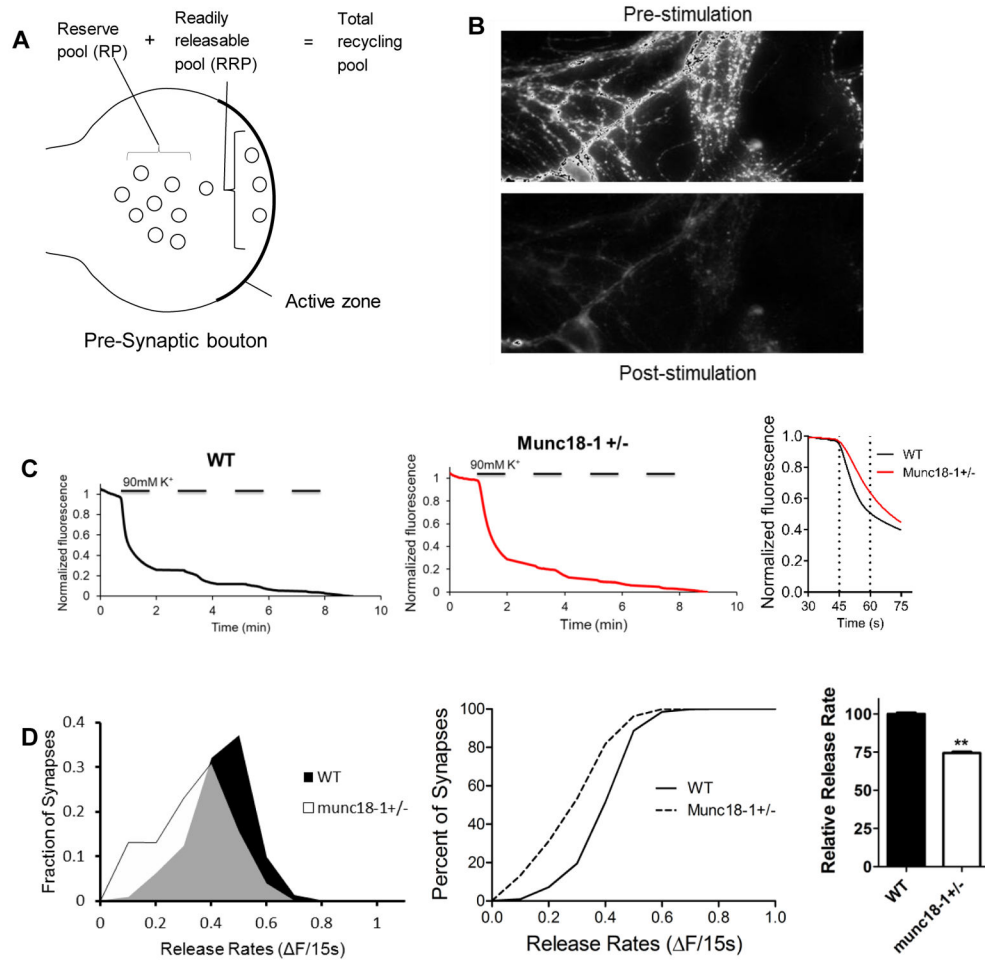


Fig. 4. Munc18^{+/-} synapses have slower vesicular release. (A) Illustration of the different synaptic pools in the presynaptic terminal. (B) Representative visualization of the loaded dye in the synapses showing fluorescence before and after the procedure. (C) Representative traces of WT and munc18-1^{+/-} neurons showing the loss of fluorescence during the experiment and comparing WT and munc18-1^{+/-} destaining rates for the first 15 s after destaining. (D) Fractional distribution and cumulative histogram showing the rate of synaptic vesicle release in the first 15 seconds as the change in fluorescence vs percentage of synapses. The graph depicts that munc18-1^{+/-} (n=10; 1292 synapses) have a slower release rate than WT (n=8; 923 synapses) neurons (p<0.001; Kolmogorov-Smirnov test). Bar graph indicates munc18-1^{+/-} neurons release approximately 25% less fluorescence than WT during that period.

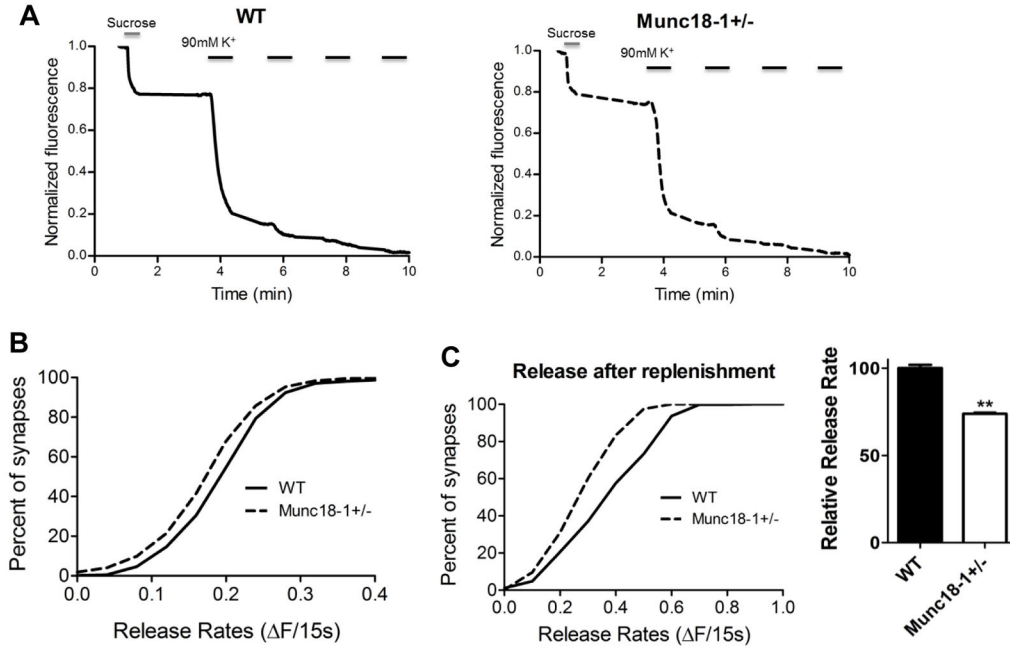


Fig. 5. Decreased readily releasable pool (RRP) of synaptic vesicles in *munc18*^{+/-} mice. (A) Representative traces of fluorescence loss during the procedure. High sucrose Tyrode solution is used to drive release during the first destaining. (B) Cumulative histogram showing *munc18-1*^{+/-} (n=13; 1516 synapses) neurons have a smaller readily releasable pool size when compared to WT (n=5; 602 synapses) (p<0.001 Kolmogorov-Smirnov test). (C) panels depict the cumulative distribution of synaptic release during high K⁺ stimulation 90 seconds after sucrose application (left); bar graph reveals that *munc18-1*^{+/-} neurons released approximately 26% less fluorescence than WT neurons (normalized to 100%) during that period (p<0.001, two tailed t-test)